

PAPER • OPEN ACCESS

Behaviour of square FRP-Confined High-Strength Concrete Columns under Eccentric Compression

To cite this article: Ali Fallah Pour *et al* 2018 *IOP Conf. Ser.: Mater. Sci. Eng.* **301** 012058

View the [article online](#) for updates and enhancements.

Related content

- [Confinement of NORMAL- AND HIGH-STRENGTH CONCRETE by Shape Memory Alloy \(SMA\) Spirals](#)
- [Numerical simulation on the mechanical behaviour of angle steel-encased composite column filled with steel tube-reinforced concrete](#)
- [MEMS-based sensors for post-earthquake damage assessment](#)

Behaviour of square FRP-Confined High-Strength Concrete Columns under Eccentric Compression

Ali Fallah Pour, Aliakbar Gholampour, Junai Zheng, Togay Ozbakkaloglu

School of Civil, Environmental and Mining Engineering, University of Adelaide,
South Australia 5005, Australia
togay.ozbakkaloglu@adelaide.edu.au

Abstract. This paper presents the results of an experimental study on the effect of load eccentricity on the axial compressive behaviour of carbon fibre-reinforced polymer (CFRP)-confined high-strength concrete (HSC) columns with a square cross-section. The axial loading was applied to the specimens at six different load eccentricities ranging from zero to 50 mm. The results show that the load eccentricity significantly influences the axial load-displacement and axial stress-strain behaviour of FRP-confined HSC. Increasing the load eccentricity leads to an increase in the ultimate axial strain but a decrease in the ultimate axial stress and second branch slope of the axial stress-strain curve.

1. Introduction

It is now well known that the strength [1-4] and ductility [5-7] of concrete can be significantly increased by lateral confinement of concrete with fibre-reinforced polymer (FRP) tubes. A large number of experimental [8-10] and analytical [11-15] studies have been performed to date to understand the compressive behaviour of FRP-confined concrete. Although over 110 models have been developed to predict the axial stress-strain relationship of FRP-confined concrete, the majority of these models were concerned with the behaviour of FRP-confined concrete under concentric compression [16].

As most of columns in real structures experience eccentric axial loading, there is need for investigating the behaviour of concrete columns under this loading condition (i.e. combination of compression and bending loading). A review of the literature shows that most of experimental studies on eccentric compression have been performed on the behaviour of FRP-confined concrete columns with internal reinforcement [17–21] and there is only a single study on FRP-confined concrete with square cross-section and without internal reinforcement [22]. Furthermore, the existing study focused on normal-strength concrete (NSC). As previously discussed in detail [23-25], high-strength concrete (HSC) is now being used in various structural applications owing to its advantages over NSC. Therefore, it is vital to determine the behaviour of FRP-confined HSC columns under eccentric compression through additional experimental studies.

This paper presents the results of an experimental study on the effect of load eccentricity on the compressive behaviour of FRP-confined HSC columns with square cross-sections using six different eccentricities ranging from zero to 50 mm. The sectional analysis conducted based on the experimental measurements was used to determine the axial stress-strain curves under eccentric loading.



2. Test Program

2.1. Test Specimens and Materials

Square columns with 150 mm cross-section and 300 mm height were prepared and confined with FRP tubes manufactured with eight layers of carbon FRP (CFRP) with a fiber layer thickness of 0.165 mm, elastic modulus of 230 GPa, and ultimate tensile strength of 4730 MPa. Specimens were designed with rounded corners with a radius of 30 mm to maintain relatively high confinement efficiency. The crushed basalt with a 10 mm nominal maximum size was used as the coarse aggregate. The HSC mix contained a polycarboxylic ether polymer-based superplasticizer and silica fume, and it had a water-to-binder ratio of 0.3, which resulted in a test day compressive strength of 105 MPa.

2.2. Instrumentation and Testing Procedure

Load eccentricity was applied to specimens by two pin supports mounted at top and bottom of the specimens at different eccentricities, including 0, 10, 20, 30, 40, and 50 mm. The specimens were tested using a 5000-kN capacity universal testing machine under axial compression initially with load control at a rate of 3 kN/sec and subsequently with displacement control at a rate of 10 microstrain/sec beyond initial softening until specimen failure. To measure the axial deformations of the specimens, two methods were used: 1) four linear variable displacement transformers (LVDTs) mounted at the corners of steel loading and supporting steel plates (full-height LVDTs); and 2) four LVDTs mounted at the mid-height of the specimens (mid-height LVDTs).

3. Test Results

3.1. Failure Mode

The concrete specimens tested under an eccentricity of 20 mm or lower failed abruptly by tube rupture with an explosive sound. On the other hand, the failure of the specimens subjected to a higher eccentricity happened with FRP tube rupture at corners or their vicinity at the compression side, while separations were observed on the FRP tube among the horizontal FRP layers around the mid-height region of the specimen on the tension side. In most specimens, the rupture of the FRP tube occurred at the mid-height of the specimen.

3.2. Axial Load-Displacement and Stress-Strain Curves

Figure 1 shows the axial load-displacement curves of specimens under different eccentricities (e). As can be seen in the figure, the load eccentricity significantly influenced the behaviour of FRP-confined HSC. It can be seen in Fig. 1 that the ultimate axial load and corresponding axial displacement measured at the point of loading decreased with an increase in the load eccentricity. These reductions are as expected and attributed to the presence of bending moments under load eccentricity and their increase with an increase in the load eccentricity.

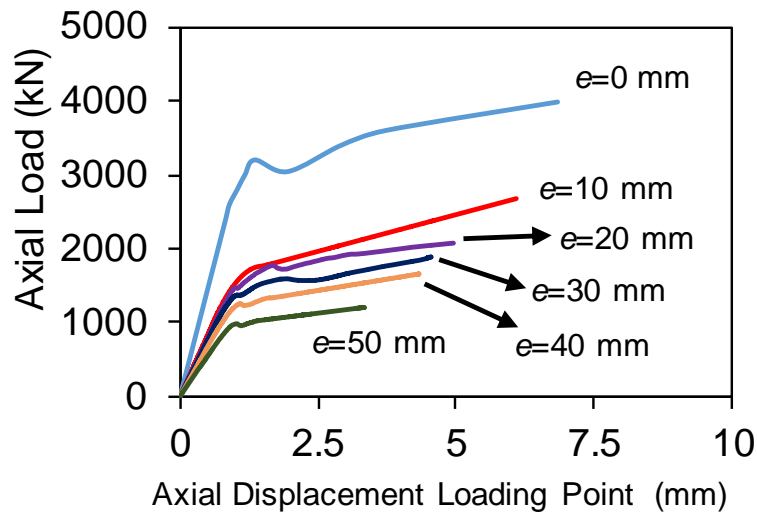


Figure 1. Axial load-displacement curves of concretes under eccentricity.

To produce the axial stress-strain curves of FRP-confined HSC under eccentric loading, sectional analysis was conducted on the recorded experimental axial load-displacement data. Figure 2 illustrates the obtained axial stress-strain curves. In the figure, E_2 , ϵ_{ct} , and f_{ct} are the second branch slope, strain at the transition point (which marks the beginning of the second portion of the stress-strain relationship), and axial stress at the transition point of the stress-strain curve, respectively. As can be seen in the figure, load eccentricity had a significant influence on the axial stress-strain curves of FRP-confined HSC. It can be seen in Fig. 2 that an increase in the load eccentricity resulted in an increase in the ultimate axial strain (ϵ_{cu}) but a decrease in E_2 , which translated to a reduced ultimate axial stress (f_{cu}). It can also be seen in the figure that f_{ct} decreased slightly in the presence of the load eccentricity. It is notable that, owing to the significant effect of the eccentricity on the axial stress-strain behaviour, existing concentric axial stress-strain models of FRP-confined concrete would not be able to accurately capture the behaviour of FRP-confined concrete under eccentric compression.

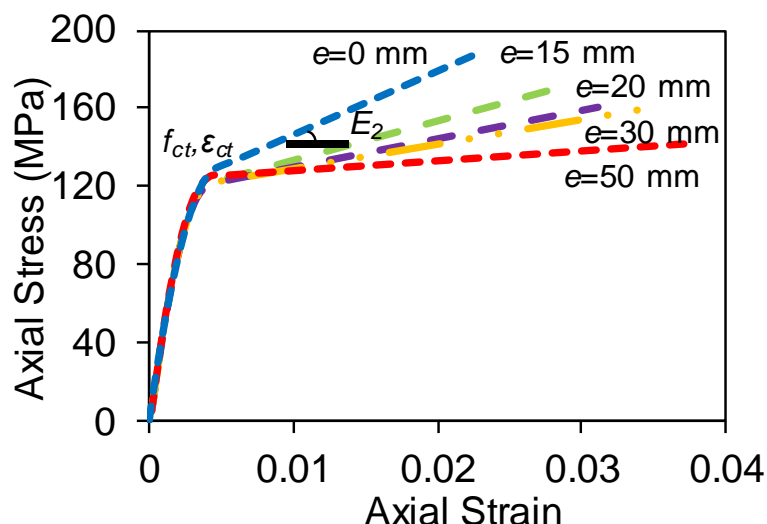


Figure 2. Axial stress-strain curves of FRP-confined concrete under load eccentricity.

Figures 3(a) and 3(b) show the variation of the normalized ultimate axial strain ($\epsilon_{cu}/\epsilon_{cu,0}$, where $\epsilon_{cu,0}$ is the ultimate axial strain of the specimens under concentric loading) and normalized ultimate axial stress ($f_{cu}/f_{cu,0}$, where $f_{cu,0}$ is the ultimate axial stress of the specimens under concentric loading) with

normalized eccentricity (e/R , where R is the cross-sectional radius), respectively. As can be seen in the figures, ε_{cu} increased and f_{cu} decreased almost linearly with an increase in the load eccentricity.

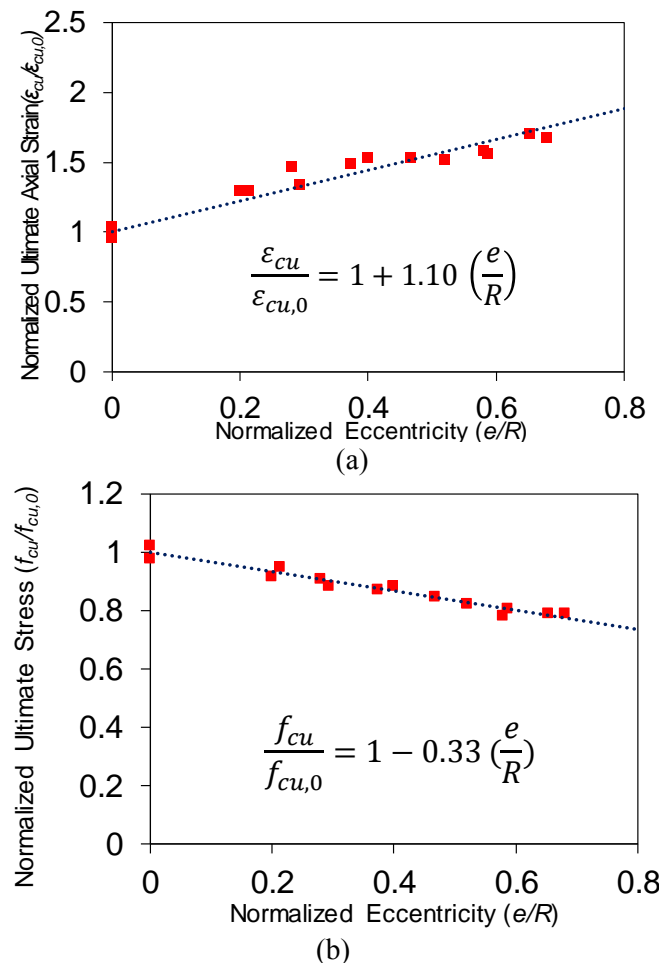


Figure 3. Variation of normalized ultimate axial (a) strain and (b) stress ratio with normalized eccentricity.

4. Conclusions

An experimental study on the axial compressive behaviour of FRP-confined square HSC columns under eccentric compression loading has been presented. The results showed that load eccentricity significantly affects the axial load-displacement curve of FRP-confined HSC. An increase in the load eccentricity leads to an increase in the ultimate axial strain but a decrease in the second branch slope of the axial stress-strain relationship, which leads to a reduced ultimate axial stress. Because of the relatively significant influence of the load eccentricity on the stress-strain behaviour of FRP-confined concrete, caution is required when applying the concentric stress-strain models of FRP-confined concrete to predict the behaviour of members under load eccentricity.

5. Acknowledgements

The authors gratefully acknowledge the financial support from the National Natural Science Foundation of China through Grant No. 51650110495 and the University of Adelaide through a Research Excellence Grant awarded to the fourth author. The authors would like to thank Mr. Gu, who contributed to the experimental procedures presented in this paper as part of his Master's study. This research is part of an ongoing program at the University of Adelaide on FRP-concrete composite columns.

6. References

- [1] Lim J C and Ozbakkaloglu T 2016 *J. Mater. Civil Eng.* **28(2)** 06015010.
- [2] Lim J C, Ozbakkaloglu T, Gholampour A and Bennett T 2016 *J. Struct. Eng.* 10.1061/(ASCE)ST.1943-541X.0001589.
- [3] Mansouri I, Gholampour A, Kisi O and Ozbakkaloglu T 2016 *Neural. Comput. Appl.* 10.1007/s00521-016-2492-4.
- [4] Vincent T and Ozbakkaloglu T 2016 *Mater. Struct.* **49(4)** 1245-1268.
- [5] Lim J C and Ozbakkaloglu T 2015 *Mater. Struct.* **48(9)** 2839-2854.
- [6] Vincent T and Ozbakkaloglu T 2017 *J Compos Constr.* 10.1061/(ASCE)CC.1943-5614.0000802.
- [7] Vincent T and Ozbakkaloglu T 2015 *J. Compos. Constr.* **19(6)** 04015003.
- [8] Ozbakkaloglu T and Vincent T 2014 *J. Compos. Constr.* 10.1061/(ASCE)CC.1943-5614.0000410.
- [9] Xie T and Ozbakkaloglu T 2015 *Eng. Struct.* **90**, 158–171.
- [10] Lim J C and Ozbakkaloglu T 2015 *Constr. Build. Mater.* **82** 61–70.
- [11] Rousakis T, Rakitzis T and Karabinis T 2012 *J. Compos. Constr.* **16(6)** 615–625.
- [12] Ozbakkaloglu T, Lim J C and Vincent T 2013 *Eng. Struct.* **49** 1068–1088.
- [13] Lim J C and Ozbakkaloglu T 2014 *J. Compos. Constr.* 10.1061/(ASCE)CC.1943-5614.0000536.
- [14] Ozbakkaloglu T, Gholampour A, Lim J C 2016 *J. Compos. Constr.* 10.1061/(ASCE)CC.1943-5614.0000712.
- [15] Keshtegar B, Ozbakkaloglu T and Gholampour A 2016 *Eng. Comput.* 10.1007/s00366-016-0481-y.
- [16] Lim J C and Ozbakkaloglu T 2014 *J. Compos. Construct.* **18(4)** 04013058.
- [17] El Maaddawy T 2009 *J. Compos. Constr.* **13(1)** 13-24.
- [18] Hajsadeghi M and Alaei F J 2010 *In Proc of the 5th International Conference on FRP Composites in Civil Engineering (CICE)*, Beijing, China 27-29.
- [19] Sadeghian P and Rahai A R and Ehsani M R 2010 *J. Compos. Constr.* **14(4)** 443-450.
- [20] Elwan S K and Rashed A S 2011 *Struct. Eng. Mech.* **39(2)** 207-221.
- [21] Quiertant M and Clement J L 2011 *Constr. Build. Mater.* **25(2)** 452-460.
- [22] Csuka B and Kollar L P 2012 *Compos. Struct.* **94(3)** 1106-1116.
- [23] Vincent T and Ozbakkaloglu T 2013 *Compos. Part B.* **50** 413-428.
- [24] Ozbakkaloglu T and Lim J C 2013 *Compos. Part B.* **55** 607-634.
- [25] Xie T and Ozbakkaloglu T 2016 *Construct. Build. Mater.* **105** 132-143.